DMD2021-1030

IMAGING OF FOCUSED ULTRASOUND-INDUCED SHEAR WAVES TO PROBE MECHANICAL ANISOTROPY OF TISSUE

Charlotte A Guertler
Washington University in St. Louis
St. Louis, MO

Ruth J Okamoto
Washington University in St. Louis
St. Louis, MO

Joel R Garbow
Washington University in St. Louis
St. Louis, MO

Hong Chen
Washington University in St. Louis
St. Louis, MO

Philip V Bayly
Washington University in St. Louis
St. Louis, MO

ABSTRACT

It is important to understand mechanical anisotropy in fibrous soft tissues because of the relationship of anisotropy to tissue function, and because anisotropy may change due to injury and disease. We have developed a method to noninvasively investigate anisotropy, based on MR imaging of harmonic ultrasound-induced motion (MR-HUM), using focused ultrasound (FUS) and magnetic resonance elastography (MRE). MR-HUM produces symmetric, radial waves inside a tissue, which enables a simple assessment of anisotropy using features of the resulting shear wave fields. This method was applied to characterize ex vivo muscle tissue, which is known to exhibit mechanical anisotropy. Finite element (FE) simulations of the experiment were performed to illustrate and validate the approach. Anisotropy was characterized by ratios of apparent shear moduli and strain components in different directions.

Keywords: Magnetic Resonance Elastography, Focused Ultrasound, Anisotropy, Experiment, FE Simulation

NOMENCLATURE

μ_1 shear modulus parallel to fiber direction
μ_2 shear modulus perpendicular to fiber direction
E_{aa} fiber strain
E_{bb} non-fiber strain
E_{ac} fiber shear strain
E_{bd} non-fiber shear strain

1. INTRODUCTION

Fibrous biological tissues are structurally and mechanically anisotropic [1]. It is important to understand the magnitude and effects of tissue anisotropy because it may modulate mechanisms of injury and disease. Measuring anisotropy is still an area of active research due to challenges associated with obtaining sufficient data to estimate anisotropy from a single sample. The objective of this study was to develop and apply a simple, robust method to probe anisotropy in fibrous soft tissues.

Shear waves can be used to assess material properties of soft tissues. Magnetic resonance elastography (MRE) is now commonly used for non-invasive estimation of tissue material properties, under the assumption they are isotropic [2-5]. MRE measures the phase-encoded displacement due to shear waves in harmonically oscillating soft tissue. The shear wave field is "inverted" to determine the stiffness of the tissue. Anisotropic parameter estimation has been performed, but it requires data from multiple shear waves within the region of interest [6].

It is challenging to obtain a rich dataset of shear waves because conventional actuation methods do not provide controlled motion in multiple directions. Actuation at an external boundary (i.e., the skull or skin) can induce multiple waves, but wave fields are uncontrolled and inconsistent in direction [7-8]. Direct actuation of tissue (i.e., with a penetrating needle) can provide controlled, symmetric wave fields, but this method is invasive and can be destructive so only one direction of wave field can be obtained in one sample [9].

Focused ultrasound (FUS) can be used to noninvasively produce shear waves in tissue through acoustic radiation force at the ultrasound focus (Fig. 1A) [10]. It has been used in many techniques, including acoustic radiation force imaging and harmonic motion imaging [10-12].

Here we use FUS in conjunction with MRE to investigate the anisotropy of tissues. This approach, termed MR imaging of harmonic ultrasound-induced motion (MR-HUM), uses low frequency, amplitude-modulated FUS to produce harmonic shear waves that propagate spherically from the focus of the ultrasound transducer (Fig 1 B). This controlled propagation of shear waves provides the data-rich wave fields necessary to examine tissue anisotropy.
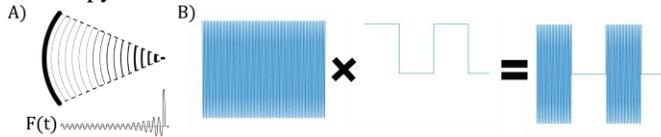

FIGURE 1: SCHEMATIC DIAGRAM OF FUS MODULATION FOR MR-HUM. (A) ULTRASOUND WAVES ARE FOCUSED TO CREATE CONCENTRATED ACOUSTIC RADIATION FORCE AT A POINT. (B) DIAGRAM OF AMPLITUDE MODULATION USED IN MR-HUM. HIGH FREQUENCY (~1.5 MHZ) ULTRASOUND WAVES ARE MODULATED USING A LOW FREQUENCY (200-600 HZ) SQUARE WAVE. THIS PROVIDES AN AMPLITUDE MODULATED FORCE THAT CAN PRODUCE HARMONIC SHEAR WAVES AT THE SQUARE-WAVE FREQUENCY.

2. MATERIALS AND METHODS

2.1 Experiment

MR-HUM was performed on 25.4 mm dia. cylinders of chicken breast (fibrous muscle) embedded in gelatin/glycerol (Fig. 2 A-B). The sample and ultrasound transducer (1.5 MHz, IGT, Pessac, France) were placed inside the bore of a 4.7T MR scanner. The ultrasound transducer was placed on the circumference of the sample (Fig. 2 C).
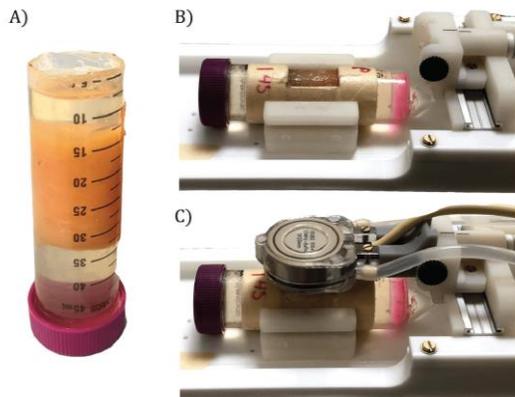

FIGURE 2: EXPERIMENTAL SETUP FOR MR-HUM OF FIBROUS SOFT TISSUE. (A) CYLINDRICAL SECTION OF EX VIVO MUSCLE (CHICKEN BREAST) EMBEDDED IN GELATIN / GLYCEROL. (B) SAMPLE IN MR COIL SHOWING TUBE CUTOUT. (C) US TRANSDUCER PLACED OVER SAMPLE.

Amplitude-modulated focused ultrasound waves were generated using low frequency square waves, inducing a local, periodic body force at either 400Hz (n=9) or 500Hz (n=4) inside

the sample (Fig. 3 A). Two excitation frequencies were used in this study to investigate if properties of the tissue were frequency-dependent. Samples were aligned with approximate fiber direction 90° to the actuation direction and analysis was performed within an 8mm radius of the US focus (Fig. 3 B-C). A custom MRE sequence was used to measure shear wave displacement components [9]. Diffusion tensor imaging (DTI) was used to estimate fiber direction in the samples from the direction of maximal diffusivity [13].
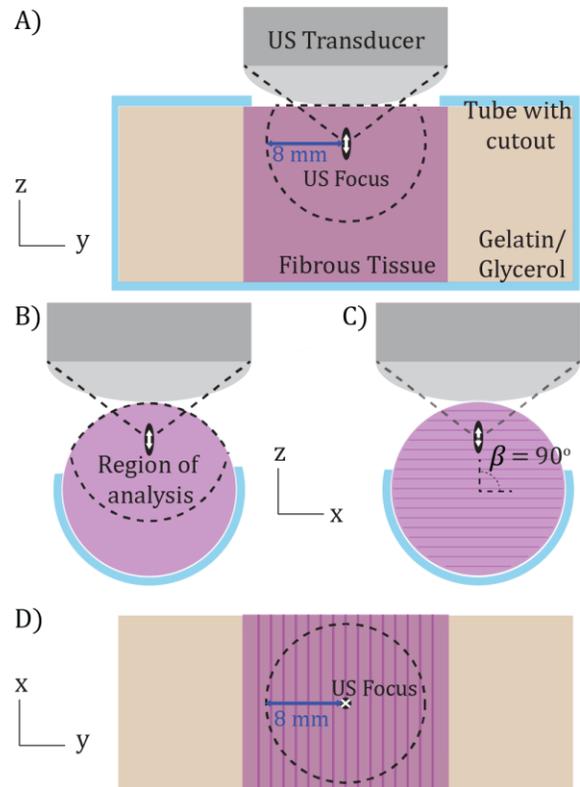

FIGURE 3: SCHEMATIC DIAGRAM OF MR-HUM IN FIBROUS TISSUE SAMPLE. (A) DIAGRAM OF SAMPLE IN Y-Z PLANE. DOTTED CIRCLE REPRESENTS REGION OF ANALYSIS. (B) DIAGRAM IN Z-X (AXIAL) PLANE SHOWING REGION OF ANALYSIS. C) DIAGRAM IN Z-X (AXIAL) PLANE SHOWING FIBER DIRECTION AT 90° RELATIVE TO THE ACTUATION DIRECTION (ALONG Z-AXIS). D) DIAGRAM IN X-Y PLANE SHOWING THE SLICE PLANE THROUGH THE US FOCUS. MR IMAGING WAS PERFORMED ALONG THIS PLANE. DOTTED CIRCLE REPRESENTS THE REGION OF ANALYSIS ON THIS SLICE. FIGURES 4-7 (EXPERIMENT AND SIMULATION RESULTS) SHOW DATA FROM THIS REGION ONLY.

2.2 Simulation

A finite element model (COMSOL Multiphysics; v. 5.4, Stockholm, Sweden) of a nearly-incompressible transversely isotropic cylinder was used to simulate MR-HUM in anisotropic tissue. The data from these simulations were used to validate and assess MR-HUM for anisotropic parameter estimation.

The simulation domain was a cylinder of linear, elastic, nearly incompressible, homogenous material, 27 mm diameter

and 50 mm length (dimensions chosen to match experimental samples). The simulation incorporated a muscle-like shear modulus of $\mu_2 = 6000\ Pa$ and a ratio between shear moduli $\mu_1/\mu_2 = 2$. A harmonic body load at 400 Hz was applied in the z-direction to a small spherical region of 1 mm radius, at the cylinder center. The steady state response was found using COMSOL's frequency domain solver. The domain consisted of 100,505 quadratic Lagrange elements, corresponding to 432,883 degrees of freedom. Data from these simulations, which are discretized but noise-free, representing an idealized scenario, were used to evaluate the method to estimate the anisotropy ratio.

Analysis of the simulations were performed on data from the spherical region within 8 mm radius of the center of the cylinder (location of the harmonic body load) to eliminate effects of wave dissipation and reflections from boundaries. All voxels outside of this region were masked out.

3. RESULTS

In the MR-HUM experiment, 3D displacement components (U, V, W, respectively) in the x-, y-, and z-directions were calculated from the MRE phase (Fig. 4). Radially propagating waves are observed for all samples in the W-component of displacement. Wave fronts are typically elliptical with the major semi-axis aligned with the fiber direction estimated from DTI.

These experimental observations were confirmed in the simulations, which also displayed elliptical waves in the W-component. The U- and V-components of displacement in the simulation were also similar to those in experiment.
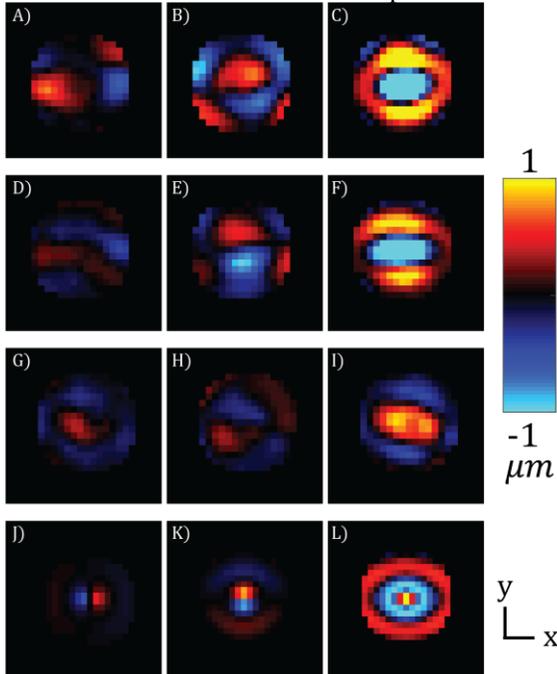
FIGURE 4: DISPLACEMENT COMPONENTS (U, V, W) FROM MH-HUM, IN ONE SLICE (X-Y PLANE) OF FIBROUS TISSUE WITH FIBER DIRECTION ALONG THE X-AXIS. (A-C) EXPERIMENT SAMPLE 1 (400 HZ); (D-F) EXPERIMENT SAMPLE 2 (400 HZ); (G-I) EXPERIMENT SAMPLE 3 (500 HZ); (J-L) SIMULATION (400 HZ).

The curl field in polar coordinates was calculated from the displacement field. The circumferential (θ) component of curl was used to isolate contributions of radially-propagating shear waves (Fig. 5 A). Local frequency estimation (LFE) was used to estimate the wave speed and apparent shear modulus (estimated from the square of the wave speed) of the samples from the θ-component of curl and the W-component of displacement (Fig. 5B) [14]. Apparent shear modulus increased with the frequency of tissue vibration (Fig 5). The θ-component of curl (Γ_θ) also displayed elliptical patterns about the focus, with the major semi-axis aligned with the fiber direction estimated from DTI. Apparent shear modulus estimates varied relative to the fiber direction, with tissue appearing stiffer within $\pm 15°$ of the fiber axis (Fig. 5). Similar trends were observed in the simulation.
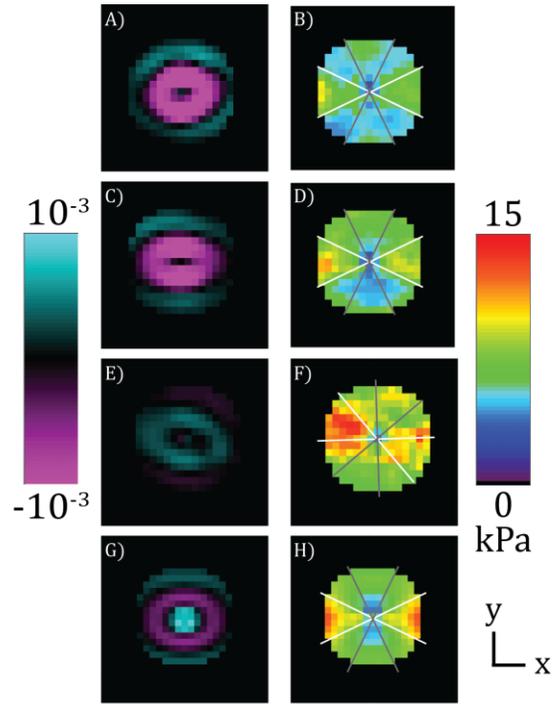
FIGURE 5: θ-COMPONENT OF CURL (Γ_θ) FOR ONE SLICE THROUGH THE US FOCUS (LEFT). (RIGHT) APPARENT SHEAR MODULUS (μ) CALCULATED BY LFE OF THE θ-COMPONENT OF CURL. WHITE LINES OUTLINE THE AREA USED TO ESTIMATE THE APPARENT SHEAR MODULUS PARALLEL TO THE FIBER DIRECTION (μ_1). GRAY LINES OUTLINE THE AREA USED TO ESTIMATE THE APPARENT SHEAR MODULUS PERPENDICULAR TO THE FIBER DIRECTION (μ_2). (A-B) EXPERIMENT SAMPLE 1 (400 HZ); (C-D) EXPERIMENT SAMPLE 2 (400 HZ); (E-F) EXPERIMENT SAMPLE 3 (500 HZ); (G-H) SIMULATION (400 HZ, SHEAR MODULUS $\mu_2 = 6000\ Pa$ AND SHEAR MODULUS RATIO $\mu_1/\mu_2 = 2$).

Strain was calculated from the displacement fields. Tensile strain in the fiber direction (E_{aa}), tensile strain in a perpendicular "non-fiber" direction (E_{bb}), shear strain in the plane containing the fibers and the applied force vector (E_{ac}), and shear strain in a perpendicular "non-fiber" plane (E_{bd}) were estimated from the

strain tensor and fiber direction vector. Strain fields displayed directional dependence, with higher values of both tensile strain and shear strain in the non-fiber directions compared to the fiber directions (Fig. 6 A-D).
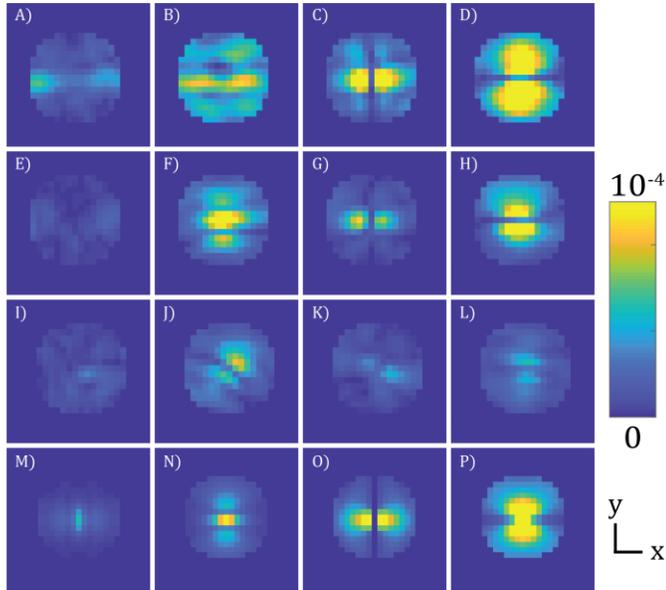

FIGURE 6: FIBER AND NON-FIBER STRAIN FIELDS FOR ONE SLICE THROUGH THE US FOCUS. FROM LEFT TO RIGHT: FIBER STRAIN FIELD (E_{aa}); NON-FIBER STRAIN FIELD (E_{bb}); FIBER SHEAR STRAIN FIELD (E_{ac}); NON-FIBER SHEAR STRAIN FIELD (E_{bd}). (A-D) EXPERIMENT SAMPLE 1 (400 HZ); (E-H) EXPERIMENT SAMPLE 2 (400 HZ); (I-L) EXPERIMENT SAMPLE 3 (500 HZ); (M-P) SIMULATION (400 HZ).

Ratios of apparent shear moduli from LFE and ratios of strains along the fiber and non-fiber directions were used to quantify the effects of anisotropy (Fig. 7). Anisotropy ratios of apparent shear modulus were calculated using the angular sectors outlined in Fig 5B. Strain ratios were taken within the hemi-spherical region of interest containing the focus and below. All samples showed various degrees of anisotropy. Corresponding anisotropy ratios from the simulation are also included in Fig. 7 (red circles).
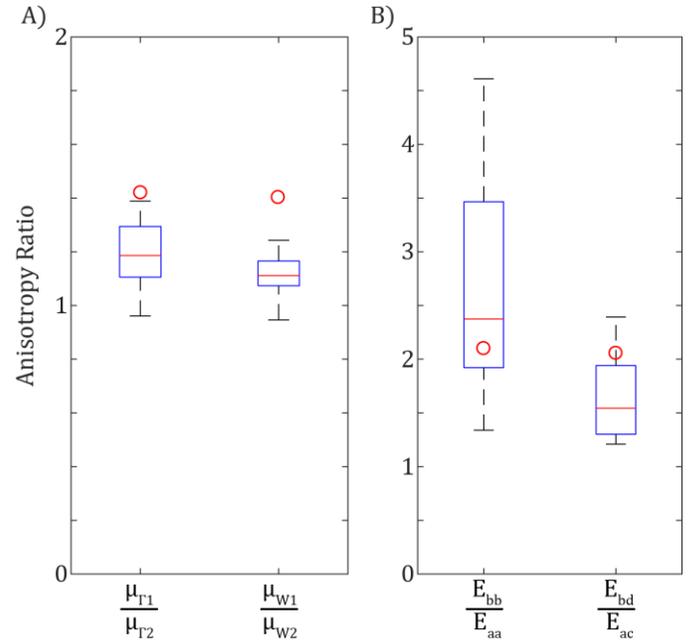

FIGURE 7: ANISOTROPY METRICS FROM MR-HUM. (A) RATIOS OF APPARENT SHEAR MODULI IN SECTORS PARALLEL AND PERPENDICULAR TO FIBERS, CALCULATED FROM LFE OF θ-COMPONENT OF CURL (μ_Γ) AND W-COMPONENT OF DISPLACEMENT (μ_w). (B) RATIOS OF NON-FIBER/FIBER TENSILE STRAIN (E_{bb}/E_{aa}) AND NON-FIBER/FIBER SHEAR STRAIN (E_{bd}/E_{ac}). CORRESPONDING METRICS OF ANISOTROPY FROM SIMULATION ($\mu_2 = 6000\ Pa$, $\mu_1/\mu_2 = 2$) ARE SHOWN BY RED CIRCLES.

4. DISCUSSION

Three different measures of mechanical anisotropy are discussed in this paper: (i) the ratio of apparent shear moduli from LFE; (ii) the ratio of tensile or shear strain in fiber and non-fiber directions; and (iii) ratio of elastic moduli. Although all three measure the mechanical anisotropy of the material, they are not equivalent. The anisotropy ratios of apparent shear moduli from LFE in different angular sectors are comparable to ratios of shear moduli from prior studies in muscle tissue. The ratio of shear moduli in chicken breast was previously estimated to be 1.8 ± 0.3 [13] from relative speeds of shear waves. Ratios of anisotropic shear moduli in turkey breast were previously estimated to be 1.6 ± 0.3 using dynamic shear testing (DST) and 2.3 ± 0.7 using traditional MRE [9]. The current LFE-based anisotropy ratios (~1.2) from MR-HUM are similar in magnitude, though smaller, than those prior estimates of shear anisotropy. In contrast, the ratios of strain in fiber and non-fiber directions (~1.5 – 2.5) from MR-HUM are close to the previous ratios of elastic moduli. The large standard deviations and spread of anisotropy values from previous methods (DST and MRE) demonstrate the complexity of anisotropic parameter estimation compounded by biological variability. "Ground truth" material parameters are very difficult to obtain, especially for biological soft tissues, which makes it important to compare results to simulations and among multiple approaches.

5. CONCLUSION

MR-HUM was developed to characterize anisotropic behavior of soft tissue. It is a non-invasive and non-destructive method that produces simple, but rich shear wave fields that can be analyzed quantitatively. MR-HUM can be readily simulated for comparison to experiment and validation of anisotropy estimates. This novel method thus can provide robust, non-invasive characterization of important mechanical characteristics of fibrous soft tissue.

REFERENCES

[1] Humphrey, J. D. et al. Determination of a Constitutive Relation for Passive Myocardium: II.—Parameter Estimation, 1990.

[2] Sack, I. et al. The impact of aging and gender on brain viscoelasticity, 2009.

[3] Sinkus, R. et al. Viscoelastic shear properties of in vivo breast lesions measured by MR elastography, 2005.

[4] Klatt, D. et al. Noninvasive assessment of the rheological behavior of human organs using multifrequency MR elastography: a study of brain and liver viscoelasticity, 2007.

[5] Sack, I. et al. The Influence of Physiological Aging and Atrophy on Brain Viscoelastic Properties in Humans, 2011.

[6] Tweten, D. J. et al. Estimation of material parameters from slow and fast shear waves in an incompressible, transversely isotropic material, 2015.

[7] Johnson, C. L. et al. Viscoelasticity of subcortical gray matter structures, 2016.

[8] Badachhape, A. A. et al. The Relationship of Three-Dimensional Human Skull Motion to Brain Tissue Deformation in Magnetic Resonance Elastography Studies, 2017.

[9] Schmidt, J. L. et al. Magnetic resonance elastography of slow and fast shear waves illuminates differences in shear and tensile moduli in anisotropic tissue, 2016.

[10] Chen, H. et al. Harmonic motion imaging for abdominal tumor detection and high-intensity focused ultrasound ablation monitoring: an in vivo feasibility study in a transgenic mouse model of pancreatic cancer, 2015.

[11] Nightingale, K. R. et al. On the feasibility of remote palpation using acoustic radiation force, 2001.

[12] Konofagou, E. E. et al. Harmonic Motion Imaging (HMI) for Tumor Imaging and Treatment Monitoring, 2012.

[13] Guertler, Charlotte A. et al. Estimation of Anisotropic Material Properties of Soft Tissue by MRI of Ultrasound-Induced Shear Waves, 2020.

[14] Knutsson, H. et al. Local multiscale frequency and bandwidth estimation, 1994.